Functional Evaluation of Invariant Arginines Situated in the Mobile Lid Domain of Phosphoribulokinase†

Jennifer A. Runquist, David H. T. Harrison, and Henry M. Miziorko*

Department of Biochemistry, Medical College of Wisconsin, Milwaukee, Wisconsin 53226

Received August 19, 1997; Revised Manuscript Received October 21, 1997

ABSTRACT: *Rhodobacter sphaeroides* phosphoribulokinase contains four invariant arginines (R49, R168, R173, and R187). The high-resolution structure of this enzyme [Harrison, D. H. T., Runquist, J. A., Holub, A., and Miziorko, H. M. (1998) *Biochemistry* (submitted for publication)] reveals that it folds in a manner similar to that of adenylate kinase. Three invariant arginines (R168, R173, and R187) as well as arginine-186, which is conserved in prokaryotic phosphoribulokinases, have not been previously functionally evaluated. These arginine residues map within the mobile lid domain that is a distinctive feature of the adenylate kinase family of proteins. Precedent for the significant function of arginines in phosphotransferase reactions prompted substitution of glutamine for each of these three invariant arginines. Solution state characterization of the isolated mutant proteins indicated that they retained a high degree of structural integrity, as indicated by their stoichiometric binding of an alternative nucleotide substrate (trinitrophenyl-ATP) as well as the allosteric effector (NADH). Kinetic characterization indicated $>10^4$-fold diminution in V/K_{Ru5P} for R168Q, attributable to a >300-fold decrease in catalytic efficiency and an increase (∼50-fold) in $K_{m\ Ru5P}$. For R173Q, a 15-fold diminution in V_{max} and a 100-fold increase in $K_{m\ Ru5P}$ were observed. These observations implicate new components of the ribulose 5-phosphate binding site. Additionally, they confirm assignment of the mobile lid domain as part of the phosphoribulokinase active site, even though this region is well separated from other active site elements in the structure of the open form of the protein. Characterization of R186Q and R187Q mutants suggests that they influence the cooperativity of substrate binding.

Phosphoribulokinase (PRK,[1] EC 2.7.1.19) catalyzes the formation of ribulose 1,5-bisphosphate (*1*), the CO_2 acceptor in the reductive pentose phosphate cycle. Since this reaction is critical to CO_2 assimilation, the enzyme functions in a variety of autotrophic organisms and its activity is regulated. Plant and algal enzymes are regulated by a thioredoxin-mediated thiol−disulfide exchange mechanism (*2*). Specifically, the eukaryotic enzyme is activated when thioredoxin f reacts with PRK's C55 (*3*) to initiate reduction of the C16−C55 disulfide bond that accounts for the inactive form of PRK (*4*). In contrast, prokaryotic PRKs are allosterically regulated (*5*−*7*), with NADH functioning as a positive effector and AMP as a negative effector.

Several active site amino acids have been identified in PRK using solution state approaches. Protein modification approaches (*8*−*10*) have mapped both C16 and C55 within eukaryotic PRK's active site, although mutagenesis experiments (*11*) have shown that neither residue greatly influences catalytic function. In contrast, reaction chemistry is crucially dependent on prokaryotic PRK's D42 and D169 (*12*); E131 also significantly influences catalytic efficiency. While these acidic amino acids could function as activator cation ligands or as a catalytic base, precise assignments of function to each of these residues have not been made. However, a specific function in sugar phosphate substrate binding has been proposed for prokaryotic PRK's R49 (*13*) or, correspondingly, eukaryotic PRK's R64 (*14*), on the basis of the large $K_{m\ Ru5P}$ effects that are observed upon mutagenesis of this arginine.

The elucidation of a high-resolution structure for *Rhodobacter sphaeroides* PRK (*15*) not only allows the evaluation of several previous structural hypotheses but also facilitates the more focused design of new tests of structure−function correlations. Recognition of a folding motif that clearly places PRK within the adenylate kinase (AK) family of proteins prompted our scrutiny of a region corresponding to the "mobile lid" domain (*16*) of AK. In contrast to the "open" PRK structure described in ref *15*, the "closed" form of AK (containing bound nucleotide) shows that the mobile lid domain becomes positioned within close proximity of other active site elements, including consensus nucleotide binding sequences. Additionally, mutagenesis of AK mobile lid arginines (*17*, *18*) has provided strong precedent for the significant function of such residues. These observations stimulated our investigation of the remaining invariant PRK

† This work was supported by grants from the U.S. Department of Agriculture National Research Initiative Competitive Research Grants Program (Photosynthesis & Respiration; 96 35306 3448) to H.M.M. and from the Herman Frasch Foundation to D.H.T.H.

* Address for correspondence: Henry M. Miziorko, Medical College of Wisconsin, Milwaukee, WI 53226. Phone: 414-456-8437. Fax: 414-456-6510. E-mail: miziorko@post.its.mcw.edu.

[1] Abbreviations: PRK, phosphoribulokinase; Ru5P, ribulose 5-phosphate; RuBP, ribulose 1,5-bisphosphate; AK, adenylate kinase; TNP-ATP, 2′(3′)-*O*-(2,4,6-trinitrophenyl)adenosine 5′-triphosphate; IPTG, isopropyl thiogalactoside.

S0006-2960(97)02052-7 CCC: $15.00
Published on Web 02/03/1998

Table 1: Oligonucleotides Encoding Substitutions for Invariant PRK Arginines

ENZYME	OLIGONUCLEOTIDES FOR MUTAGENIC CASSETTES
Wild Type	
	162 164 166 168 170 172 174 176 178 180
	I Q K I H R D R A T R G Y T T E A
R168Q	
	GATCCAGAAGATCCACCAGGACCGCGCGACCCGCGGTTACACGACCGAGGCG
	GTCTTCTAGGTGGTCCTGGCGCGCTGGGCGCCAATGTGCTGGCTCCGCCAGTG
R173Q	
	GATCCAGAAGATCCACCGCGACCGCGCGACCCAGGGTTACACGACCGAGGCG
	GTCTTCTAGGTGGCGCTGGCGCGCTGGGTCCCAATGTGCTGGCTCCGCCAGTG
Wild Type	
	180 182 184 186 188
	A V T D V I L R R M H
R186Q	
	GTCACCGACGTGATCCTGCAGCGGATGCAT
	GCTGCACTAGGACGTCGCCT
R187Q	
	GTCACCGACGTGATCCTGCGCCAGATGCA
	GCTGCACTAGGACGCGGTCT

arginines (R168, R173, and R187) as well as R186 (conserved in prokaryotic PRKs), which are situated in PRK's mobile lid domain. The relative contributions of these residues to the PRK-catalyzed formation of RuBP are documented in this report.

MATERIALS AND METHODS

Materials. Deoxyoligonucleotides and fluorescein-labeled sequencing primers were synthesized by the Protein/Nucleic Acid Shared Facility at the Medical College of Wisconsin or purchased from Operon Technologies, Inc., and purified, as required, using C_{18} Sep-Pak cartridges from Waters. T4 DNA ligase and restriction enzymes were purchased from United States Biochemical Corp. DNA fragments were isolated using Geneclean and Mermaid kits from Bio 101 Inc. Plasmid DNA grown in JM105 *Escherichia coli* was isolated using Qiagen's plasmid mini and midi kits. DNA sequence analysis was performed using a Pharmacia/LKB ALF DNA sequencer.

For recombinant protein expression, ampicillin was purchased from Fisher Scientific and isopropyl β-D-thiogalactoside (IPTG) from Research Products International Corp. (Mt. Prospect, IL). Adenosine 5′-triphosphate, β-NADH, and D-ribulose 5-phosphate were purchased from Sigma Chemical Co. Sodium [^{14}C]bicarbonate (57.38 mCi/mmol) was a product of NEN Research Products. DTT and Tris and Hepes buffers were purchased from Research Organics, Inc. Chromatography media utilized for PRK isolation included reactive green-19 agarose from Sigma Chemical Co. and Q Sepharose Fast Flow from Pharmacia Biotech. For fluorescence experiments, TNP-ATP [2′(3′)-*O*-(2,4,6-trinitrophenyl)adenosine 5′-triphosphate] from Molecular Probes was utilized. The RuBP carboxylase required for the CO_2 fixation assay of PRK activity was isolated after expression in *E. coli* JM103 cells using a plasmid generously provided by C. R. Somerville.

Construction of prkA Mutant Alleles. The mutant alleles of prkA encoding the single-amino acid substitutions R168Q and R173Q were constructed in pETbprkwt using cassette mutagenesis and a three-way ligation strategy. First, a *Pst*I/*Bam*HI fragment of about 3.8 kb, including the 5′-end of the *prkA* gene, was isolated from pETbprkwt (*12*). Second, a *Pst*I/*Bst*EII fragment of about 1.8 kb, including the 3′-end of the gene, was isolated from a similar plasmid. This left about 60 bp of the *prkA* gene that could be replaced by the R168Q or R173Q encoding *Bam*HI/*Bst*EII cassettes (produced by annealing four synthetic oligonucleotides) displayed in Table 1.

Cassette mutagenesis was also used to produce R186Q and R187Q mutant alleles. Unique *Bst*EII and *Nsi*I restriction sites flank these two arginines so that replacement of the wild-type coding sequence with a synthetic 29 bp mutagenic cassette would accomplish the desired substitution (Table 1). To facilitate the three-way ligation protocol, the T7 expression plasmid pETbprkwt was digested with *Pst*I and *Bst*EII which produced a 1.86 kb fragment and a 3.8 kb fragment. The larger fragment, which includes the 5′-end of *prkA*, was isolated. Similarly, pETbprkwt was digested with *Pst*I and *Nsi*I again, producing a 1.8 kb fragment and a 3.8 kb fragment, but in this case, the smaller fragment, which includes the 3′-end of *prkA*, was isolated. For each mutation, a three-way ligation was performed using the *Pst*I/*Bst*EII 3.86 kb fragment, the *Pst*I/*Nsi*I 1.86 kb fragment, and the 29 bp *Bst*EII/*Nsi*I mutagenic cassette (Table 1). A three-way ligation protocol was selected over a two-way ligation protocol due to the potential for wild-type contamination in the latter protocol. For R186Q, the mutation created a *Pst*I site, which facilitated identification of the appropriately mutated plasmid. Plasmids were screened to determine that the appropriate restriction enzyme sites were still intact. DNA sequencing in both directions confirmed that the expression plasmids encoded the anticipated arginine mutations and verified that no additional mutations had been introduced.

Expression and Purification of PRK. *E. coli* BL21(DE3) cultures containing plasmid pETbprkR168Q, pETbprkR173Q, pETbprkR186Q, or pETbprkR187Q (*12*) were grown at 25 °C in 2 L of ampicillin-containing LB media to an OD_{600} of ∼0.7. Expression of PRK was induced by addition of IPTG to a final concentration of 1 mM followed by 3−4 h of additional growth. The cells were collected by low-speed centrifugation; cell pellets were suspended and disrupted using a French pressure cell. A 100000*g* supernatant was prepared and subjected to Q-Sepharose anion exchange chromatography followed by affinity chromatography on reactive green-19 agarose. PRK was eluted from reactive green-19 agarose affinity resin with a buffer containing 25 mM Tris-HCl (pH 8.2), 10 mM β-mercaptoethanol, 1 mM EDTA, and 10 mM ATP. For quantitative protein concentration estimates, an extinction coefficient of 50 303 M^{-1} cm^{-1} at 280 nm was used (*19*).

TNP-ATP and NADH Binding Stoichiometry Measurements. TNP-ATP binding to PRK was followed by fluorescence measurements utilizing an SLM 4800C spectrofluorometer. For TNP-ATP titrations in 25 mM Tris-HCl buffer (pH 8.0), the excitation wavelength was 408 nm and the emission spectra were scanned from 500 to 600 nm. For data analysis, values measured at the fluorescence emission peak of 545 nm for PRK-bound TNP-ATP were utilized (*19*). NADH binding to PRK was also measured using fluorescence methods. Emission spectra were scanned from 400 to 550 nm, using 340 nm excitation. For data analysis, values measured at the fluorescence emission peak of 440 nm for PRK-bound NADH were utilized. The binding stoichiometry of mono- and dinucleotides to PRK was determined from the intersection point of lines fit to the low-occupancy and plateau regions of the titration data by linear regression analysis (*20*). Calculated stoichiometries reflect binding sites per 32 kDa PRK subunit.

Kinetic Characterization of PRK. A radioisotopic assay that involves trapping the PRK reaction product RuBP via the RuBP carboxylase-dependent incorporation of $^{14}CO_2$ to form acid-stable [^{14}C]-3-phosphoglycerate (*21*) was utilized. In standard assays, the final concentrations of reaction mixture components were 100 mM Hepes (pH 8.0), 1 mM DTT, 20 mM $MgCl_2$, 20 mM $KH^{14}CO_3$ (∼1000 dpm/nmol), 5 mM ATP, 1 mM Ru5P, 1 mM NADH, and 100 milliunits of recombinant RuBP carboxylase. Enzyme assays were conducted at 30 °C. For kinetic characterization of the mutant proteins, ATP concentrations ranged from 0.05 to 15 mM; Ru5P concentrations ranged from 0.05 to 8 mM. Kinetic data were fit by a nonlinear regression analysis algorithm (*22*).

RESULTS

Rationale for Investigation of Invariant Arginines of PRK. Early mutagenesis work on prokaryotic PRK (*13*) was directed toward several basic residues (H45, R49, and K53) situated in a region identified as part of the active site on the basis of affinity labeling (*23*). The $K_{m\ Ru5P}$ was elevated upon elimination of basicity at R49 and also, albeit to a lesser extent, upon mutagenesis at H45. Observation of a similar effect with *Chlamydomonas* PRK (*14*) underscored the significance of these results. Binding of phosphorylated metabolite substrates to phosphotransferases frequently involves multiple active site arginines. The interactions of 3-phosphoglycerate with phosphoglycerate kinase (*24*) and fructose 6-phosphate with phosphofructokinase (*25*) illustrate this point, although those enzymes exhibit folding motifs different from that reported for PRK in ref *15*. While no structure of a 6-phosphofructo-2-kinase complex with fructose 6-phosphate is currently available, mutagenesis work (*26*, *27*) has implicated several arginines in the binding of that substrate. The kinase domain of that enzyme (*28*) resembles PRK in that both fold in a manner similar to that of adenylate kinase. This extensive precedent, as well as previous results of adenylate kinase mutagenesis (*17*, *18*), suggested that the functional evaluation of PRK's invariant R168, R173, and R187 (all of which are situated within the mobile lid domain; Figure 1) would be worthwhile. Thus, mutagenesis to eliminate basicity of R168, R173, and R187 or the flanking R186 by substituting glutamine at each of these positions was performed.

Expression, Isolation, and Structural Characterization of Mutant PRKs. pET-based expression plasmids harboring the appropriately mutated PRK-encoding DNA were transformed into *E. coli* BL21, which were propagated and induced with IPTG to stimulate PRK production. Cell extracts were prepared using a French pressure cell, and membrane-depleted supernatants were subjected to Q-Sepharose anion exchange and agarose−Reactive Green 19 affinity chromatography as described earlier (*12*). Expression levels as well as the homogeneity of preparations of these mutants were comparable to those previously demonstrated for wild-type PRK and catalytic mutants (*12*) prepared using the equivalent expression strategy.

Recently, we demonstrated (*19*) that PRK forms binary complexes with the fluorescent alternative substrate, TNP-ATP, or with the positive allosteric effector, NADH. The purified arginine mutants were tested for their ability to support stable, stoichiometric binding of these nucleotides at substrate and effector sites, respectively. Titrations of

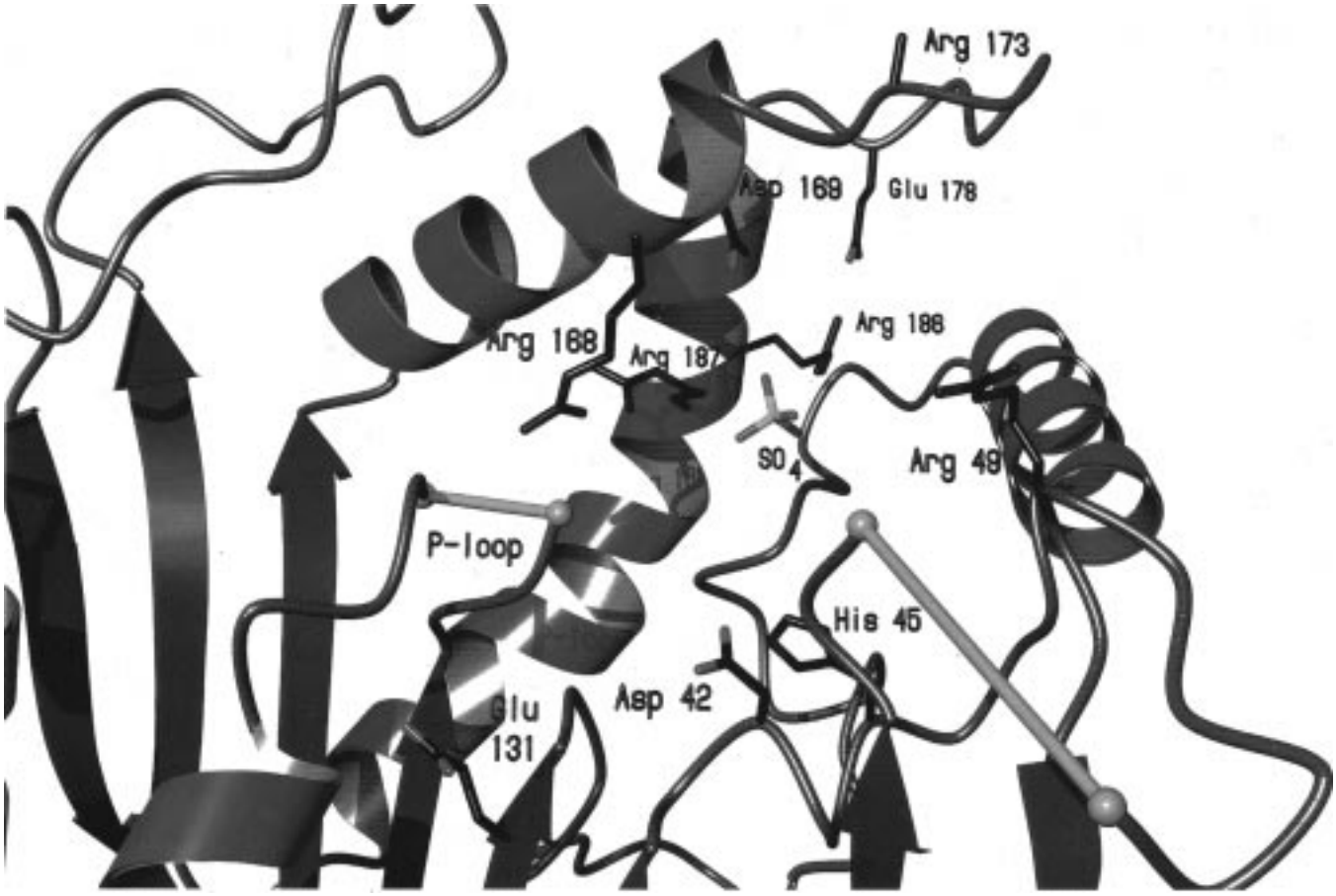

FIGURE 1: Structural representation of the *R. sphaeroides* phosphoribulokinase active site. In addition to the residues (R168, R173, R186, and R187) for which mutagenesis data are now reported, several residues (D42, H45, R49, and D169) previously implicated as part of the active site are also labeled. The figure indicates that a proposed Walker B motif (in which E131 is situated) is adjacent to a highly disordered Walker A or P-loop motif (depicted with a break in the α-carbon backbone between residues G17 and T18).

R168Q and R173Q with TNP-ATP (Figure 2) indicate that these proteins bind one molecule of this alternative substrate per 32 kDa PRK subunit; these titrations illustrate one method of verifying that the mutants contain a full complement of functional substrate sites. As shown in Table 2, extension of analogue binding studies to each of the mutant PRKs indicated that there are not substantial differences ($n = 0.8-1.1$ per site) between TNP-ATP or NADH binding stoichiometries measured for wild-type PRK and the various arginine mutants. These observations suggest that the mutants contain catalytic and effector sites that are substantially unperturbed and imply that overall tertiary structure is unaltered by the substitution of glutamine for arginine. Additionally, as might be anticipated on the basis of their ability to form binary complexes with NADH, these mutants remain sensitive to activation by this allosteric effector, suggesting that intersubunit interactions in the octameric PRKs are not disrupted.

Kinetic Characterization of Mutant PRKs. The prediction that the invariant arginines would influence the efficiency of the PRK-catalyzed reaction has been validated by experimental observations (Table 3). The predominant effect of eliminating the basic side chain by a glutamine substitution varies with each residue targeted for mutagenesis. However, none of the mutations had a major effect on ATP saturation; $S_{1/2}$ varied by <6-fold. In the case of R168Q, the $>10^4$-fold V/K effect is dominated by a >300-fold change in catalytic efficiency (Table 3); the ~50-fold elevation in $K_{m\ Ru5P}$ is a smaller but, nonetheless, substantial effect. In contrast, with R173Q, the 15-fold diminution of catalysis is overshadowed by the 100-fold increase in $K_{m\ Ru5P}$.

Table 2: Substrate and Effector Binding by PRK Mutants[a]

enzyme	$n_{TNP-ATP}$	n_{NADH}
wild type	1.0 ± 0.03	0.97 ± 0.03
R168Q	1.1 ± 0.03	0.88 ± 0.05
R173Q	0.90 ± 0.05	0.87 ± 0.05
R186Q	0.90 ± 0.04	1.1 ± 0.04
R187Q	1.1 ± 0.04	1.1 ± 0.04

[a] *n* denotes the calculated number of binding sites per enzyme subunit. Stoichiometries for TNP-ATP and NADH binding were determined from fluorescence titrations as described in Figure 2.

The significant perturbations observed with R168Q and R173Q are not accompanied by any change in shape of the substrate saturation curves (hyperbolic and sigmoidal for Ru5P and ATP, respectively). For R187Q, while there are only modest effects on substrate affinity and little change in catalytic efficiency, Ru5P saturation now exhibits a sigmoidal dependency (Hill coefficient = 2.9; Table 3). When the flanking, nonconserved R186 is mutated to glutamine, perturbations in V_{max} and substrate levels required for saturation are again modest. In contrast to wild-type PRK and the other arginine mutants, R186Q exhibits a hyperbolic (Hill coefficient = 1.0; Table 3) rather than a sigmoidal dependency for saturation by substrate ATP.

Table 3: Steady-State Kinetic Parameters of Wild-Type and Mutant PRKs[a]

enzyme	$K_{m\ Ru5P}$ (mM)	n_H	$S_{1/2\ ATP}$ (mM)	n_H	V_{max} (units/mg)
wild type	0.096 ± 0.014	(h)	0.55 ± 0.16	1.98 ± 0.15	338 ± 18
R168Q	4.6 ± 0.8	(h)	2.4 ± 0.08	1.87 ± 0.16	0.98 ± 0.14
R173Q	10.5 ± 1.5	(h)	1.5 ± 0.05	1.96 ± 0.23	22.0 ± 2.4
R186Q	0.048 ± 0.004	(h)	0.17 ± 0.02[c]	1.02 ± 0.06	273 ± 13
R187Q	0.55 ± 0.04[b]	2.9 ± 0.5	3.2 ± 0.4	2.66 ± 0.57	150 ± 8.3

[a] The $K_{m\ Ru5P}$ is the ribulose 5-phosphate concentration at half-maximal velocity, as calculated from a fit of the Ru5P saturation data to the Michaelis−Menten equation. The $S_{1/2\ ATP}$ is the ATP concentration at half-maximal velocity, as calculated from a fit of the ATP saturation data to the Hill equation. n_H is the Hill constant. (h) indicates that the kinetics are hyperbolic with respect to Ru5P. The maximal velocity, given in micromoles per minute per milligram, is estimated from the Michaelis−Menten equation fit to the Ru5P saturation data. [b] This estimate represents $S_{1/2\ Ru5P}$. [c] This estimate represents $K_{m\ ATP}$.

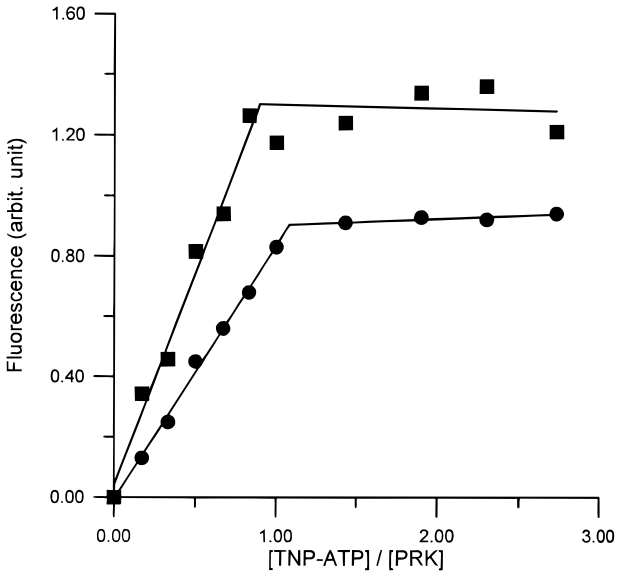

FIGURE 2: Fluorescence titration of PRKs R168Q and R173Q with TNP-ATP. Sequential additions of TNP-ATP were made to a fluorescence cuvette containing either 6.0 μM R168Q (●) or 6.0 μM R173Q (■) in 25 mM Tris-HCl (pH 8.0). The relative fluorescence enhancement is plotted versus the ratio of TNP-ATP to PRK subunit present in the cuvette. Lines fit to the data represent linear regression fits of the low- and high-occupancy data points; stoichiometry of TNP-ATP binding is determined from the intersection point of the calculated lines.

DISCUSSION

The elucidation of a high-resolution structure for PRK has provided a wealth of new information concerning this enzyme and has confirmed the significance of many observations made before these structural data became available. One side of the active site cavity (Figure 1, bottom) is defined by the interior edge of the central β-sheet. This region includes a Walker A or "P loop" motif after the end of β-strand 1, the catalytically essential Asp-42 after β-strand 2, and the invariant Glu-131 of the Walker B motif at the end of β-strand 3. The opposite side of the active site cavity is formed by the mobile lid (Figure 1, top) that includes the helix−loop−helix region in which Arg-168, Arg-173, Arg-186, and Arg-187 as well as the catalytically essential Asp-169 are situated. The observation that invariant carboxyls (D42, E131, and D169) which influence catalysis (*12*) are situated within the active site cavity provides a structural rationale for the kinetic properties of the mutants lacking these carboxyl groups. In this context, the 300-fold change in k_{cat} for R168Q invites some comparison. This effect is substantially smaller than the 10^4-10^5-fold effects measured upon mutation of D42 and D169 (*12*), but is easily comparable to that measured for E131. In all PRK sequences, there are four hydrophobic residues upstream of E131, suggesting that this glutamate represents the acidic residue of a Walker B nucleotide binding motif (*29*). Such a residue typically contributes a ligand to the cation of the M^{2+}-ATP substrate so that, in retrospect, observation of a substantial k_{cat} effect ($\sim 10^2$-fold) upon elimination of a carboxylate from this position seems reasonable. Observation of an effect of similar magnitude due to an R168Q substitution confirms the importance of the mobile lid domain's involvement as part of the active site (Figure 1). A more precise interpretation of the effect might also involve a consideration of whether R168 influences the reactivity of D169, which remains a viable candidate for the role of active site general base. However, such a discussion appears to be premature in the absence of a more definitive assignment of the function of D169.

The available PRK structure (Figure 1) corresponds to the open form of the enzyme and exhibits a large distance between certain amino acids that are expected to be more closely juxtaposed during catalytic turnover. For example, the dynamic P-loop (depicted in Figure 1 with a break in the α-carbon backbone between residues 17 and 18) is positioned adjacent to both Glu-131 of the Walker B motif and the catalytically essential Asp-42. This region of PRK is ∼15 Å from the mobile lid that includes the α-helix which contains Arg-168 and the catalytically essential Asp-169, as well as the subsequent loop in which Arg-173 is situated. This open structure complicates somewhat the interpretation of the $K_{m\ Ru5P}$ effects observed with R173Q. While K_m effects do not always correlate well with changes in affinity, effects of the type and magnitude observed for R173Q are frequently used to implicate an amino acid in substrate binding (*30*). The 10^2-fold effect observed with R173Q is comparable in magnitude to the effect previously reported for R49Q (*13*). However, it is clear that, if the K_m data are interpreted to suggest that R49 and R173 are both involved in binding of Ru5P's C5 phosphoryl group, there would have to be considerable movement of the lid domain to close the active site cavity and bring R49 and R173 into proximity. Such lid movement is well established for adenylate kinase (*16*), which folds in a manner quite similar to that of PRK. This precedent, together with the observation that these arginines are situated in the region of the AK-like active site where the phosphoryl acceptor binds (*16*, *28*), makes attractive the simplest interpretation of the $K_{m\ Ru5P}$ data for

R49Q and R173Q, i.e., assignment of these residues to the binding of Ru5P's phosphoryl group. An alternative explanation might note the significant k_{cat} effect for R173Q and suggest that changes in the catalytic terms which contribute to the magnitude of R173Q's apparent $K_{m\ Ru5P}$ influence the observed effect. Such an explanation would be in accord with participation of R173 in transition state stabilization but remains quite speculative in the absence of solution or crystal structure information on the orientation of ATP and/or Ru5P in a PRK complex that corresponds to a closed form of the protein.

Mutations that eliminate the basicity of R186 and R187 appear to influence the cooperativity of substrate binding. Since only prokaryotic PRKs exhibit allosteric effects [activation by NADH and inhibition by AMP or PEP (*5*, *6*)], subunit interactions which influence allosterism are likely to involve not the evolutionarily conserved dimeric interface but rather those interactive structural elements that are unique to the prokaryotic PRK oligomers. In this context, elimination of positive charge at R186 or R187, while not directly affecting NADH−PRK complex formation (Table 2), may impair propagation of the structural changes that elevate V_{max} and support cooperative ATP saturation of the wild-type PRK octamer.

The structural information now available for PRK has certainly provided a useful perspective with which to interpret the existing body of mechanistic and mutagenesis data. Despite this advance, ambiguities persist and prevent unequivocal assignment of certain structure−function correlations. A combination of more refined solution structure tests of function and the extension of crystallographic analyses to higher-order complexes of PRK with substrates and effectors will allow us to develop a more thorough understanding of the molecular basis for this key reaction in carbon assimilation.

REFERENCES

1. Hurwitz, J., Weisbach, A., Horecker, B. L., and Smyrniotis, P. (1956) *J. Biol. Chem. 218*, 769−783.
2. Buchanan, B. B. (1980) *Annu. Rev. Plant Physiol. 31*, 341−374.
3. Brandes, H. K., Larimer, F. W., and Hartman, F. C. (1996) *J. Biol. Chem. 271*, 3333−3335.
4. Porter, M. A., Stringer, C. D., and Hartman, F. C. (1988) *J. Biol. Chem. 263*, 123−129.
5. Rindt, K. P., and Ohmann, E. (1969) *Biochem. Biophys. Res. Commun. 36*, 357−364.
6. Abdelal, A. T. H., and Schlegel, H. G. (1974) *Biochem. J. 139*, 481−489.
7. Tabita, F. R. (1980) *J. Bacteriol. 143*, 1275−1280.
8. Porter, M. A., and Hartman, F. C. (1986) *Biochemistry 25*, 7314−7318.
9. Krieger, T. J., and Miziorko, H. M. (1986) *Biochemistry 25*, 3496−3501.
10. Porter, M. A., Potter, M. D., and Hartman, F. C. (1990) *J. Protein Chem. 9*, 445−451.
11. Milanez, S., Mural, R. J., and Hartman, F. C. (1991) *J. Biol. Chem. 266*, 10694−10699.
12. Charlier, H. A., Runquist, J. A., and Miziorko, H. M. (1994) *Biochemistry 33*, 9343−9350.
13. Sandbaken, M. G., Runquist, J. A., Barbieri, J. T., and Miziorko, H. M. (1992) *Biochemistry 31*, 3715−3719.
14. Roesler, K. R., Marcotte, B. L., and Ogren, W. L. (1992) *Plant Physiol. 98*, 1285−1289.
15. Harrison, D. H. T., Runquist, J. A., Holub, A., and Miziorko, H. M. (1998) *Biochemistry* (submitted for publication).
16. Schlauderer, G. J., Proba, K., and Schulz, G. E. (1996) *J. Mol. Biol. 256*, 223−227.
17. Yan, H., Shi, Z., Tsai, M. D., et al. (1990) *Biochemistry 29*, 6385−6392.
18. Dahnke, T., Shi, Z., Yan, H., Jiang, R. T., and Tsai, M. D. (1992) *Biochemistry 31*, 6318−6328.
19. Runquist, J. A., Koteiche, H. A., and Miziorko, H. M. (1996) *Biochemistry 35*, 9295.
20. Leatherbarrow, R. J. (1992) *GraFit Version 3.0*, Erithacus Software Ltd., Staines, U.K.
21. Paulsen, J. M., and Lane, M. D. (1966) *Biochemistry 5*, 2350−2357.
22. Marquardt, D. W. (1963) *SIAM J. Appl. Math. 2*, 431−441.
23. Miziorko, H. M., Brodt, C. A., and Krieger, T. J. (1990) *J. Biol. Chem. 265*, 3642−3647.
24. Bernstein, B. E., Michels, P. A. M., and Hol, W. G. J. (1997) *Nature 385*, 275−278.
25. Shirikihara, Y., and Evans, P. R. (1988) *J. Mol. Biol. 204*, 973−994.
26. Li, L., Lin, K., Kurland, I. J., Correia, J. J., and Pilkis, S. J. (1992) *J. Biol. Chem. 267*, 4386−4393.
27. Tsujikawa, T., Watanabe, F., and Uyeda, K. (1995) *Biochemistry 34*, 6389−6393.
28. Hasemann, C. A., Istvan, E. S., Uyeda, K., and Deisenhofer, J. (1996) *Structure 4*, 1017−1029.
29. Walker, J. E., Saraste, M., Runswick, M. J., and Gay, N. J. (1982) *EMBO J. 1*, 945−951.
30. Berger, S. A., and Evans, P. R. (1990) *Nature 343*, 575−576.

BI972052F